12-2015

Multidimensional Tensor Array Analysis of Multiphase Flow during a Hydrodynamic Ram Event

Andrew J. Lingenfelter
Air Force Institute of Technology

David Liu

Journal of Physics: Conference Series

Multidimensional tensor array analysis of multiphase flow during a hydrodynamic ram event

Multidimensional tensor array analysis of multiphase flow during a hydrodynamic ram event

A Lingenfelter and D Liu

2950 Hobson Way, Wright-Patterson AFB, OH 45433, USA

E-mail: `andrew.lingenfelter@afit.edu`

Abstract. Flow visualization is necessary to characterize the fluid flow properties during a hydrodynamic ram event. The multiphase flow during a hydrodynamic ram event can make traditional image processing techniques such as contrast feature detection and PIV difficult. By stacking the imagery to form a multidimensional tensor array, feature detection to determine flow field velocities are visualized.

1. Introduction

Fluid flow visualization is critical for quantitatively and qualitatively determining flow characteristics and properties in engineering and physics. The research community has made great strides in developing quantitative data acquisition techniques for cavitation and flow analysis such as high-speed cameras, particle image velocimetry (PIV), rapid pulse lasers for short exposure times, and increasing camera resolution [1]. During this hydrodynamic ram (HRAM) experiment, spherical steel projectiles were accelerated horizontally into a tank of water at velocities of 45 to 150 m/s. Imagery was collected at 41,025 frames per second with a 9.61 μs exposure time utilizing a brightfield imaging technique [6]. Entrained flow fields inside the cavity were detected during testing. This effort attempts to measure velocities of the entrained flow field within the cavity. However, the cavity boundary masks the entrained flow field making contrast detection of the flow field difficult via traditional methods. This paper presents a new technique using multidimensional tensors to obtain velocity measurements of the entrained flow field.

2. Objective

During an HRAM event, a cavity forms behind the projectile consisting of fluid vapor from cavitation and entrained gasses from ambient air. When characterizing HRAM, it is necessary to detect and process items of interest in the flow field [2, 3]. Utilizing high-speed imagery, the spherical projectile is clearly discernible and detection of its position was completed in prior research [4]. However, the cavity's entrained flow is visually detected, but not as easily measured through traditional techniques such as PIV.

Edge detection of the flow field's front is difficult since the contrast is masked by the cavity's gas-liquid boundary layer. Predicting the contrast gradient to detect multiple flow fronts is computationally intensive due to contrast differences and the transient nature of the flow field. However, the formation of a multidimensional tensor enables flow field detection where traditional techniques have failed. Hence the development of the "image cube" for detection and analysis of multiphase flows.

An image, $\mathrm{A_n}$ represented by Equation 1, is an $r \times c$ matrix composed of pixel values, a, from the specified image frame number, n. $\mathrm{A_n}$ represents a typical image where vertical position is on the y-axis and horizontal position is on the x-axis. An image cube, Equation 2, is a multidimensional tensor of all the images collected with frame number residing on the z-axis shown in Figure 1(a). To determine the flow field's velocity, an image slice, S_r via Equation 3 at the specified row, r, of interest is needed. The user must specify r based on the row location of the flow field of interest in $\mathrm{A_n}$. Row 130 was selected due to the proximity to the projectile shot line of which S_{130} was generated. The box placed around the image cube in Figure 1(a) corresponds to row 130 for all the images composing S_{130}. Therefore, S_{130} is a horizontal plane of the tensor and contains the frame number versus horizontal position data utilized for velocity analysis of the flow field for row 130.

$$\mathrm{A_n} = \begin{bmatrix} a_{1,1} & a_{1,2} & \cdots & a_{1,c} \\ \vdots & \vdots & \ddots & \vdots \\ a_{r,1} & a_{r,2} & \cdots & a_{r,c} \end{bmatrix} \tag{1}$$

$$\mathrm{IC} = \left[A_1 \ldots A_n\right] \tag{2}$$

$$S_r = \begin{bmatrix} \mathrm{A_{1_{(r,1)}}} & \mathrm{A_{1_{(r,2)}}} & \cdots & \mathrm{A_{1_{(r,c)}}} \\ \mathrm{A_{2_{(r,1)}}} & \mathrm{A_{2_{(r,2)}}} & \cdots & \mathrm{A_{2_{(r,c)}}} \\ \vdots & \vdots & \ddots & \vdots \\ \mathrm{A_{n_{(r,1)}}} & \mathrm{A_{n_{(r,2)}}} & \cdots & \mathrm{A_{n_{(r,c)}}} \end{bmatrix} \tag{3}$$

Vertical position and velocity analysis is possible by looking at the vertical plane of the tensor. To detect velocities in multiple directions, correlation of the flow field between the multiple tensor planes is necessary. However, the horizontal velocity is much larger than the vertical velocity in this experiment. Therefore, since the dominant flow is in the horizontal direction for this experiment, only the horizontal plane is utilized for the position and velocity data.

3. Methodology Verification

Although application of tensors for mathematical and statistical analysis is common [5], applying a multidimensional tensor for flow field analysis is unique. Therefore, utilizing a series of generated images of a target with known pixel locations, the image cube methodology was applied to verify the technique. The target had known pixel shifts of 1, 0, -3, and 10 pixels per frame in the horizontal direction. Applying Equation 3 generated the image slice seen in Figure 2. The slope of the lines located in regions 1 through 4 represent the respective 1, 0, -3, and 10 pixel per frame shifts of the target in the generated images, confirming the original known velocity of the target.

4. Results

Row 130 was selected to generate S_{130} for HRAM data analysis due to its proximity to the projectile shot line. Using Figure 3(a), the first and darkest contrast line represents the projectile as it traverses the camera's field of view. The next contrast line is representative of the first entrained flow field and is highlighted by line 1. Line 1 begins at row 37, horizontal position 443 and is represented by $S_{130_{(37,443)}}$. $S_{130_{(37,443)}}$ corresponds to row 130, horizontal position 443 of frame number 37 represented by $A_{37_{(130,443)}}$ and shown in Figure 3(b). The contrast line is followed to $S_{130_{(51,235)}}$ which corresponds to $A_{51_{(130,235)}}$ shown in Figure 3(c). Comparison between the contrast line from the image cube to the raw imagery, it is apparent the image cube is sufficient at detecting the entrained flow field. Line 1's slope is indicative of the velocity and is equal to 14.9 pixels per frame–corresponding to a flow field entrainment velocity of 119.4 m/s.

Further analysis of Figure 3(a) indicates additional contrast lines for flow field analysis. The velocity of the entrained flow fields are summarized in Table 1. These additional contrast lines

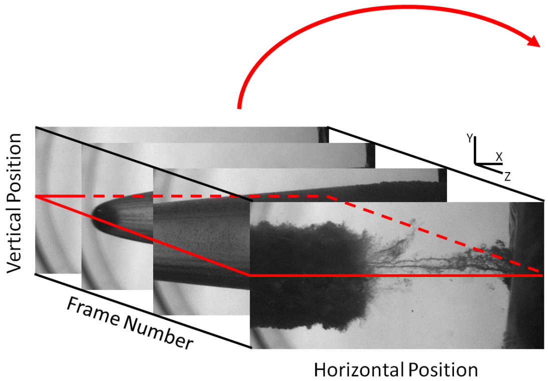

(a) Image Cube

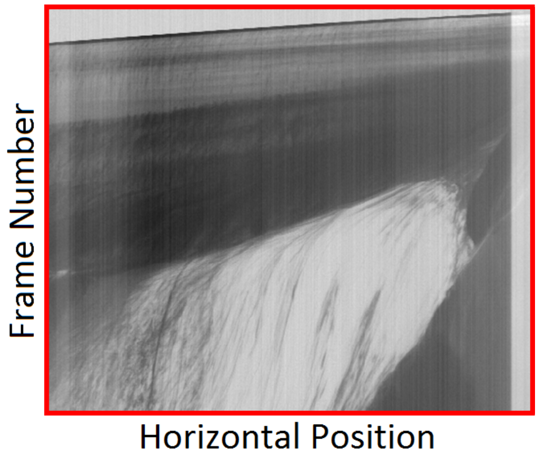

(b) Slice 130 (S_{130}) of Image Cube

Figure 1: A visual example of how the tensor is formed to create the image cube for flow analysis. Notice, instead of positional depth on the the z axis, Frame Number is on the z axis. This subtle difference is not instinctive but is important to conduct position and velocity analysis at the desired S_r. S_{130} corresponds to row 130 of all images collected and formed together via Equation 3 to obtain Frame Number vs. Horizontal Position information. Time is obtained by using the frame number and the known camera's frame rate.

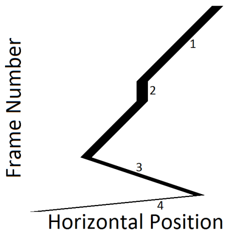

Figure 2: An example of an image slice from generated imagery of a target with known pixel positions. Regions 1, 2, 3, and 4 correspond to the square moving at 1, 0, -3, and 10 pixels per frame, respectively.

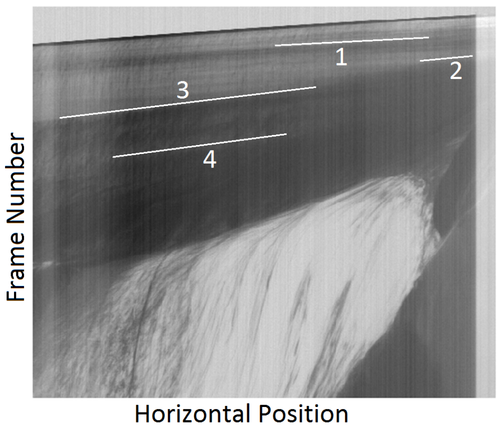

(a) Slice 130 (S_{130})

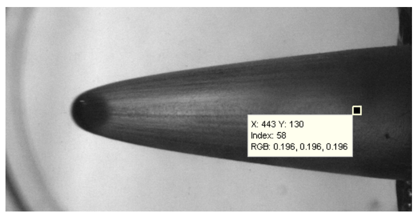

(b) Point 1 - Frame 37

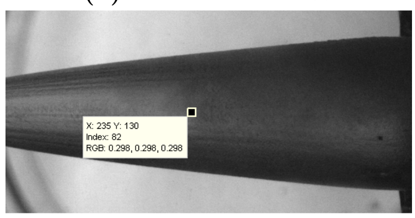

(c) Point 2 - Frame 51

Figure 3: Slice 130 of the image cube used to detect and characterize the entrained flow field velocity. Figure 3(b) and Figure 3(c) correspond to line 1 in Figure 3(a).

were chosen for a variety of reasons. Line 3 is representative of detecting a flow field with a lower velocity than the flow field represented by line 1. Line 2 represents calculating a flow field entrainment very close to the projectile penetration orifice. Lines 2 and 4 also exemplify calculating a flow field velocity in a heavily masked region.

In comparison, the PIV software utilized an adaptive correlation technique to determine the pixel shift between frames in a specified subset region of the image. Since the flow is not seeded, correlation between frames utilizes the pixel contrast to determine the shift between the subset regions. When the PIV software did detect the flow field, the average of the PIV vectors in the subset region is within the same order of magnitude as the calculated velocity from the image cube. In some cases, the entrained flow field was not detected by the PIV software even though the flow field is visually observed in the raw imagery. As stated earlier, the cavity boundary masks the entrained flow field making the contrast difficult to detect and correlate between frames for the PIV software. Lines 2 and 4 are examples when the PIV software was not able to detect the flow field velocity, yet application of the imagery cube methodology at S_{130} was able to provide these measurements.

Table 1: Measured entrainment velocities derived from Figure 3(a) for a projectile impact velocity of 146 m/s.

Reference Lines from Figure 3(a)	Calculated Velocity from image cube (m/s)	Average Velocity from PIV software (m/s)
1	119.4	91.0
2	109.8	Software did not detect
3	59.9	45.5
4	53.2	Software did not detect

5. Conclusion

The methods presented here detail the ability of processing flow data utilizing a multidimensional tensor array. Application of this technique to calculate flow velocities in multiple directions requires additional development. However, where traditional techniques have failed, utilization of this technique was able to provide useful velocity calculations for flow field characterization in a multiphase flow during an HRAM event.

6. Acknowledgments

The authors thank Dr. Matthew Fickus for the helpful discussion about image processing techniques, and for collaborating on the method used here. We also would like to thank Eric Brickson, Scott Wacker, Patrick O'Connell, and all the 96^{th} Test Group, AVSF for their experimental assistance.

References

[1] Noel T. Clemens. Flow imaging. *Encyclopedia of Imaging Science and Technology*, 2002.
[2] Peter J Disimile, Luke A Swanson, and Norman Toy. The hydrodynamic ram pressure generated by spherical projectiles. *International Journal of Impact Engineering*, 36(6):821–829, 2009.
[3] Nicolas Lecysyn, Aurlia Bony-Dandrieux, Laurent Aprin, Frdric Heymes, Pierre Slangen, Gilles Dusserre, Laurent Munier, and Christian Le Gallic. Experimental study of hydraulic ram effects on a liquid storage tank: Analysis of overpressure and cavitation induced by a high-speed projectile. *Journal of Hazardous Materials*, 178(13):635 – 643, 2010.
[4] Andrew J. Lingenfelter and David Liu. Development of methods for characterizing hydrodynamic ram cavity dynamics. AIAA, 2015.
[5] Douglas C Montgomery. *Design and analysis of experiments*, volume 7. Wiley New York, 1984.
[6] Gary S. Settles. Schlieren and shadowgraph techniques for fluid physics experiments - a brief tutorial. 2008.